

Role of eddies on organic matter production and f -ratios in the Bay of Bengal

V.V.S.S. Sarma^{1,2}, K. Yadav¹, S. Behera²

¹CSIR-National Institute of Oceanography, Regional Centre, Visakhapatnam, India

²Academy of Scientific and Innovative Research, Dona Paula, Goa, India

Abstract

In order to examine the sources of nutrients and f -ratios in the cyclonic (CE) and anticyclonic eddy (ACE), the content and isotopic composition of carbon and nitrogen in suspended particulate organic matter (POM) were analyzed in one CE and two ACEs in the western Bay of Bengal (BoB). Relatively higher concentrations of Chlorophyll- a (Chl- a) and nutrients were observed in the CE and no-eddy (NE) regions than ACE region. Higher concentrations of particulate organic carbon (POC) and nitrogen (PN) were observed in the CE and NE than ACE in the BoB. Isotope mixing model (SIAR) suggested that POM pool mainly consists of marine plankton biomass (~80%) and contribution of terrestrial organic matter is insignificant (<20%). The depth of nitracline was shallower in the CE due to divergence while it was deeper in the ACEs due to convergence of upper ocean. The isotopic composition of nitrogen in the POM varied between 2.4 and 8.5‰ and relatively lower values were associated with deeper nitracline depth in the ACE and vice versa in the CE. This suggests that upward mixing of subsurface nitrate supported primary production in the CE and regenerated nitrogen in the ACE region. The estimated f -ratios using $\delta^{15}\text{N}_{\text{POM}}$ and depth of nitracline were almost double in the CE (0.31 ± 0.04) and NE (0.28 ± 0.05) than ACEs (0.19 ± 0.09) in the BoB. Though upward mixing of subsurface low DO water intensified oxygen minimum zone (OMZ) below 75 m in the CE region, enhanced phytoplankton biomass and its export may further intensify. In contrast, convergence of DO rich surface water and low f -ratios in the ACE resulted in weaker OMZ. This study suggests that eddies significantly influence primary and export productions that may lead to modifications in intensity of OMZ in the BoB. More than 50 eddies form every year in the BoB and its impact on primary and export production leading to intensification/weakening of OMZ should be evaluated using both observations and models.

1. Introduction

Suspended particulate organic matter (POM), consists of phytoplankton, bacteria, zooplankton, plays a significant role on marine carbon and nitrogen cycle (Saino and Hattori, 1980). Due to their vertical transport to deeper depths, the atmospheric carbon dioxide (CO_2) is removed from the surface layer and also supports organic carbon demand to the heterotrophs dwelling at the deeper depths. The source of nutrients determines the magnitude of organic matter formation and their subsequent sink to deeper depths. The isotopic composition of nitrogen in POM ($\delta^{15}\text{N}_{\text{POM}}$) provides an insight on source and transformations of nutrients in the water column. The $\delta^{15}\text{N}_{\text{POM}}$ has a strong dependence on the $\delta^{15}\text{N}$ of sources of nitrogen (atmospheric N_2 , NO_3^- and NH_4^+). Several studies were carried out in the global ocean to identify possible source of nutrients using $\delta^{15}\text{N}_{\text{POM}}$ (Wada and Hattori, 1980; Saino and Hattori, 1980; Altabet, 1996; Sarma et al., 2014; Sherin et al., 2018).

Increase in biological production were reported in the regions of mesoscale eddies and fronts in the global ocean in the observational studies (eg. Strass, 1992; Denman and Abbott, 1994) as well as in the numerical models (eg: Levy et al., 1998; Oschlies and Garcon, 1998; Mahadevan and Archer, 2000). Eddies are found to be significant source of nutrients to the euphotic zone and increase new as well primary productions (McGillicuddy et al., 2003; Chelton et al., 2011; Gaube et al., 2014; Doblin et al., 2016). Based on high spatial resolution models, it was observed that cyclonic eddies (CE) are source of nutrients to the photic zone and anticyclonic eddies (ACE) are sink in the Atlantic Ocean (McGillicuddy et al., 2003). Eddies not only increase new production but also modify microbial species composition in the upper ocean (McGillicuddy, 2016; Doblin et al., 2016) due to modification in nutrients and organic matter inputs. Substantial offshore transport of carbon and nutrients by eddies were also observed in the California Current System (Nagai et al., 2015).

Prasanna Kumar et al. (2004) found that injection of subsurface nutrients to surface resulted in 3 folds increase in primary production in the CE in the Bay of Bengal (BoB). In addition to this, significant increase in sinking carbon fluxes to deeper depths was also observed associating with CEs in the BoB (Vidya and Prasanna Kumar, 2013). On the other hand, ventilation of nutrient poor and oxygen rich waters to subsurface waters in the ACE leads to weakening of oxygen minimum zone (OMZ) in the BoB (Sarma et al., 2013; 2016; Sarma and Uday Bhaskar, 2018).

BoB harbors one of the high sinking carbon flux regions to the deeper waters in the world ocean (Sarma et al., 2006) and it was attributed to ballasting of river-borne organic matter (Ittekkot et al., 1991). Recently Anand et al. (2018) observed that heterotrophs consume most of the primary produced organic matter in the upper ocean and only <2% of primary production reaches to the 100

m depth. In contrast, f -ratios, estimated based on tracer incubation experiments, are high in the BoB (0.54 to 0.72) even compared to the highly productive Arabian Sea (0.15 to 0.82) (McCarthy et al., 1999; Kumar et al., 2004; Kumar and Ramesh, 2005; Gandhi et al., 2010). The high regeneration of organic matter (Anand et al., 2018) and high f -ratios (Gandhi et al., 2010) are contradictory to each other suggesting that either alternative source of nutrients may be possible in the BoB or estimation of f -ratios may need re-evaluation.

Recently Sherin et al. (2018) estimated f -ratios in the BoB using $\delta^{15}\text{N}_{\text{POM}}$ in the mixed layer and found that relatively higher f -ratios in the CE and cyclone-influenced regions than other regions sampled in the BoB during November-December 2013. This suggests that physical processes, such as eddies, may support high phytoplankton production in the BoB through bringing nutrient-rich waters to the surface. Based on the 17 years of remote sensing sea surface height and surface currents data, it was reported that ~ 10 eddies per 1° grid were formed in the BoB between 1992 and 2009 (Chen et al., 2012; Dandapath and Chakraborty, 2016). Therefore, source of nutrients and organic matter production may be significantly modified by eddies in the BoB. We hypothesized that higher amount of POM may be produced within the CE as divergence brings subsurface nutrients to surface whereas less POM is produced in the ACE due to support of phytoplankton production by regenerated nutrients. In order to test this hypothesis, two ACEs, one CE and one no-eddy (NE) regions were studied in the western BoB.

2. Material and methods

2.1. Sampling and methods

A cruise was undertaken in the BoB along the east coast of India, covering one CE, two ACEs and NE regions during 23 March to 6 April 2018 (Fig. 1). Water column temperature, salinity (SBE 911 plus, USA), fluorescence (Wet Labs, USA) and DO (SBE 43, USA) were measured using sensors attached to Rosette (SBE 32, USA). The accuracies of these sensors are ± 1.0 db, $\pm 0.001^\circ\text{C}$, ± 0.002 psu, ± 0.01 mg m^{-3} and ± 2 μM respectively. The sampling was carried out in the upper 500 m of water column at standard depths using 10 L Niskin bottles attached to the CTD Rosette. We reported here only data collected in the upper 100 m. Water samples from the Niskin bottles were subsampled for DO analysis into 60 ml glass stoppered bottles and care was taken to avoid trapping of air bubbles. The DO was measured using Winkler titration method following potentiometric detection (Carritt and Carpenter, 1966) using potentiometer (Titrande Metrohm, Zofingen, Switzerland). A 2-L water sample was filtered through a GF/F filter (0.7 μm pore size; Whatman) and Chl-*a* retained on the filter was first extracted with N,N-dimethyl formamide (DMF), at 4° C in the dark for 12 h and

then spectrofluorometrically analyzed (Varian Eclipse fluorophotometer) following Suzuki and Ishimaru (1990). The analytical precision for Chl-*a* analysis was $\pm 0.04 \text{ mg m}^{-3}$. The DO and fluorescence data collected by sensors were calibrated with measured DO and Chl-*a* and the slope was close to one (0.98 and 0.96 respectively) and the appropriate corrections were applied. The concentrations of nutrients were measured following standard spectrophotometric procedures using an autoanalyzer (Technicon; Taacs, Australia) (Grasshoff et al. 1983). The detection limits for nitrate, and ammonium were ± 0.02 , and $\pm 0.05 \text{ }\mu\text{M}$, respectively. Total suspended matter (TSM) was determined by dry weight of the material retained on a $0.22 \text{ }\mu\text{m}$ polycarbonate filter (Millipore) after filtering ca. 2 to 5 L of water under a moderate vacuum.

POM was obtained by filtering 5 to 10 L of water through a pre-combusted (400°C , 12 h) $0.7 \text{ }\mu\text{m}$ GF/F filter (Whatman) under a gentle vacuum. For isotopic analyses of particulate organic carbon (POC), the filters were exposed to fumes of concentrated hydrochloric acid in a desiccator for overnight, followed by drying in an oven at 60°C , to remove traces of inorganic carbon. The dried filter was directly used for stable carbon isotope analysis of particulate organic carbon (POC). A sub sample of the filter without acid treatment was used directly for particulate nitrogen (PN) content as the acid treatment significantly alters N isotopic composition (Goering et al., 1990; Bunn et al., 1995; Pinnegar and Polunin, 1999). The content and stable isotopes of POC and PN were measured using an elemental analyzer (Flash EA, Thermo) coupled to an isotope ratio mass spectrometry instrument (IRMS; Delta V plus; Thermo Electron, Germany) via a ConFlo IV interface. Content is reported as $\mu\text{g/l}$ and stable isotope ratios in δ notation calculated as follows.

$$\delta R = \left(\frac{X_{sam}}{X_{std}} - 1 \right) \times 1000 \text{ ‰}$$

Where, R represents ^{13}C for carbon (C) and ^{15}N for nitrogen. X_{sam} is $^{13}\text{C}/^{12}\text{C}$ and $^{15}\text{N}/^{14}\text{N}$ of sample for C and N respectively. Similarly, X_{std} denotes $^{13}\text{C}/^{12}\text{C}$ and $^{15}\text{N}/^{14}\text{N}$ of standard for C and N respectively. The IAEA standards and internal standards, such as glutamic acid, alanine, and Organic Analytical Standard (OAS), were used for calibration. The long term precision of the instrument is about $\pm 0.2\text{‰}$ for both C and N.

Atmospheric aerosols (referred as total suspended particulates (TSP)) were collected onboard research vessel along the cruise track on pre-combusted quartz fiber filters (PALLFLEX) using High Volume Sampler (Envirotech 430) at a flow rate of $1.2 \text{ m}^3 \text{ min}^{-1}$. Nutrients in the aerosols were

measured using Ion Chromatography (850 Metrohm Professional, Switzerland) following the method described by Yadav et al. (2016).

N^* was computed following Gruber and Sarmiento, (1997) using the following equation:

$$N^* = (N - 16P + 2.90) \times 0.87 \quad (1)$$

Where N and P are dissolve nitrate and phosphate (in μM) respectively.

The depth of mixed layer (MLD) was estimated by first estimating density at *in situ* temperature, salinity and pressure and subtract 0.5°C from the temperature profile and estimate density again. The depth of MLD is taken where the difference in density of the *in situ* temperature and 0.5°C becomes zero following Shankar et al. (2015).

2.2. Quantification of organic matter contribution from various sources

The relative contribution of terrestrial organic matter in the study region was quantified using isotope mixing model “SIAR” (Stable Isotope Analysis in R). This model resolves contribution of various sources within a Bayesian framework (Parnell et al., 2010). SIAR model uses Markov Chain Monte Carlo method, and produces probable fraction of different sources. The end-members of possible sources are taken as soil organic matter from Ganges river basin (-25.0‰ and 2.5‰ for carbon and nitrogen respectively), detritus from C_3 plants ($-28.5 \pm 0.8\text{‰}$ and $2.4 \pm 0.5\text{‰}$), C_4 plants ($-13.1 \pm 1.2\text{‰}$ and $3.4 \pm 2.1\text{‰}$) and marine phytoplankton ($-23.9 \pm 0.6\text{‰}$ and $6.2 \pm 0.3\text{‰}$) respectively for carbon and nitrogen. The isotopic end-members of C_3 and C_4 land plant detritus was taken from Krishna et al. (2014) who collected samples from the various regions in the Indian subcontinent.

2.3. Satellite Data

Sea surface height anomaly (SSHA; $0.25 \times 0.25^\circ$ degree) and Geostrophic currents ($0.25 \times 0.25^\circ$ degree; Merged product) obtained from Copernicus Marine Environmental Monitoring Service (www.marine.copernicus.eu). In order to identify the region of origin and its track of advection to the sampling region, daily SSHA data were analysed and the track of each eddy were plotted (Supplementary Fig. S1; Sarma et al., 2018). This analysis suggested that CE was formed in the northeastern BoB on 12 January 2018 (about two and half months prior to sampling) and advected to the sampling region. The northern ACE (ACE_N) was formed in the northeastern BoB on 24 September 2017 about 6 months prior to our sampling. The southern ACE (ACE_S) was formed in the eastern BoB on 1 December 2017 about 4 months prior to our sampling (Fig. S1; Sarma et al., 2018). The SSHA variability on the day of each station was also plotted to examine which part of the eddy was sampled (Supplementary Fig. S2). The eddy is identified based on the circulation of water and

SSHA. If the SSHA is positive and higher than 0.2 m and anticyclonic circulation occurs, this region is identified as ACE and vice versa for CE.

Results

3.1. *Impact of eddies on hydrographic properties of water column*

Both temperature and salinity in the upper 100 m of water column increased from north to south along transect (Fig. 2a,b). Occurrence of low saline water was observed in the upper 20 and 60 m of water column in the CE and ACE_N regions respectively and its influence was decreased towards NE and ACE_S (Fig 2a). The depth of 22 isopycnal density layer showed significant spatial variation with shallow (~55 m) under the influence of CE compared to ACE_N (90 m) and ACE_S (~80 m) and NE regions (~60 m). Similarly, ~34.0 of salinity was observed at >100 m in the ACE_N and 82 m in the ACE_S than that of 50-60 m in the CE and NE regions (Fig. 2b). The MLD varied between 6.5 and 34.5 m in the study region and it was shallower in the CE (~15±4 m) than ACE (32±6 m) (Fig. 2a).

3.2. *Impact of eddies on biogeochemical properties of water column*

Relatively higher concentration of Chl-*a* in the upper ocean (mean of upper 50 m) was observed in the CE region (0.35 mg m⁻³) than NE (0.22 mg m⁻³), ACE_N (0.11 mg m⁻³) and ACE_S (0.10 mg m⁻³; Fig. 2c; Table 1). The depth integrated Chl-*a* (up to 100 m) was higher in the CE (34.6 mg m⁻²) compared to NE (26.4 mg m⁻²), ACE_N (23.6 mg m⁻²) and ACE_S (22.2 mg m⁻²) regions. The prominent subsurface Chl-*a* maximum was observed at a depth of 20 to 30 m, but it was weaker below ACE than CE and NE regions (Fig. 2c). Dissolved oxygen (DO) concentration in the upper 100 m followed the thermocline with relatively higher concentrations in the upper 100 m of water column (150-185 µM) in the ACE_N and ACE_S whereas <75 µM were observed in the CE regions at the depth below 50 m (Fig. 2d).

Upsloping of higher nitrate isolines from subsurface was noticed in the CE and NE regions whereas downsloping was observed in the ACE_N and ACE_S regions (Fig. 3a). Relatively higher nitrate concentration (2-5 µM) was observed in the upper 40 m of water column in the CE region whereas it was <1 µM in the ACE regions. The mean concentrations of nitrate in the upper 50 m were 1.98 µM in the CE and it was 1.58 µM in the NE and 0.02 and 0.12 µM in the ACE_N and ACE_S respectively (Table 1). The depth of 2 µM nitrate isoline was close to surface in the CE and NE regions and the same was deepened to 80 m in the ACE_N and ACE_S regions (Fig. 3a). Relatively higher concentration of ammonium was observed in the ACE (0.5-1.0 µM) than CE region (<0.2 µM) in the upper 50 m of water column. N* varied between -2.7 and 2.6 µM in the mixed layer and higher

concentrations ($>0 \mu\text{M}$) were observed in the north associated with low salinity whereas $<0 \mu\text{M}$ was observed in the rest of the study region (Supplementary Figure S3).

3.3. Spatial variations in content and isotopic composition of carbon and nitrogen in the BoB

The concentrations of POC varied between 44.4 and $214.8 \mu\text{g l}^{-1}$ in the upper 100 m of water column. Relatively higher POC concentrations were observed in the CE ($158.5 \pm 10 \mu\text{g l}^{-1}$) and NE ($132.0 \pm 3 \mu\text{g l}^{-1}$) than ACE (92.4 ± 9 and $88.1 \pm 8 \mu\text{g l}^{-1}$ respectively in the ACE_N and ACE_S; $t_{\text{stat}}=3.13$; $p<0.001$). Below the mixed layer also relatively higher concentrations were observed in the north than south (Fig. 4a). The concentrations of PN varied between 0.24 and $30.2 \mu\text{g l}^{-1}$ in the study region and relatively lower values were observed in the ACE (6.9 ± 2 and $8.5 \pm 3 \mu\text{g l}^{-1}$ in the ACE_N and ACE_S respectively) than CE ($22.5 \pm 2 \mu\text{g l}^{-1}$; $t_{\text{stat}}=8.74$; $p<0.001$) (Fig. 4b). Both mixed layer mean Chl-*a* and depth integrated Chl-*a* (upper 100 m of water column) showed significant linear relation with PN ($r^2=0.63$; $p<0.001$) and POC ($r^2=0.54$; $p<0.001$; Fig. 5). The concentration of PN and POC did not show any relationship with salinity ($r^2=0.00$). The concentration of TSM was relatively higher in the northern BoB mainly in the CE region ($5.6 \pm 0.9 \text{ mg l}^{-1}$) compared to other regions (4.0 to 4.3 mg l^{-1} ; Table 1). The C/N ratio was relatively lower and close to Redfield ratio in the CE (8.6 ± 2) and NE (8.0 ± 2) than ACEs (17.2 ± 4 and 10.8 ± 3 in the ACE_N and ACE_S respectively). The POC:Chl-*a* ratio varied between 430 and 2217 (mean 1123 ± 389) in the entire study region.

The isotopic composition of carbon in POM ($\delta^{13}\text{C}_{\text{POM}}$) ranged from -27.2 to -19.7‰ in the study region with mean of $-24.4 \pm 2\text{‰}$ (Fig. 4c). Relatively lighter values were observed in the CE ($-25.3 \pm 0.4\text{‰}$) than ACE_N ($-24.2 \pm 0.3\text{‰}$) and ACE_S ($23.4 \pm 0.4\text{‰}$) (Table 1). The $\delta^{13}\text{C}_{\text{POM}}$ displayed significant inverse relation with concentration of POC in the mixed layer ($r^2=0.34$; $p<0.001$; Fig. 5). The isotopic composition of nitrogen in POM ($\delta^{15}\text{N}_{\text{POM}}$) ranged between 2.4 and 8.5‰ in the upper 100 m of water column (Fig. 4d). The $\delta^{15}\text{N}_{\text{POM}}$ value is close to $\delta^{15}\text{N}_{\text{NO}_3}$ in deep water in the CE ($5.8 \pm 0.2\text{‰}$) and NE ($5.0 \pm 0.4\text{‰}$) and depleted values were found in the ACEs (4.0 ± 0.4 and $3.7 \pm 0.5\text{‰}$ in the ACE_N and ACE_S respectively). The $\delta^{15}\text{N}_{\text{POM}}$ showed significant relation with neither PN concentrations nor salinity in the mixed layer.

3.4. Spatial variations in total suspended particulate matter (TSP) in the atmosphere

The TSP in the atmosphere varied between 9.6 and $20.6 \mu\text{g m}^{-3}$ above the study region with relatively higher concentrations in the north ($16.9 \pm 3 \mu\text{g m}^{-3}$) than south ($9.9 \mu\text{g m}^{-3}$). The concentration of nitrate in the TSP varied from 0.08 to $0.28 \mu\text{gN m}^{-3}$ with insignificant spatial variations. Relatively higher concentrations of nitrate were observed in the TSP over CE (0.23 ± 0.07

$\mu\text{g m}^{-3}$), followed by NE ($0.15\pm 0.04 \mu\text{g m}^{-3}$), ACE_S ($0.15\pm 0.03 \mu\text{g m}^{-3}$) and ACE_N ($0.09\pm 0.01 \mu\text{g m}^{-3}$).

4. Discussions

4.1. Spatial variations in sources of POM and nutrients in the BoB

The variability in the PN (0.24 to $30.22 \mu\text{g l}^{-1}$) and POC (44.4 to $214.8 \mu\text{g l}^{-1}$) in the BoB is within the range expected in the marine environment (Kumar et al., 2005; Aumont et al., 2017; Sherin et al., 2018). Relatively higher PN and POC were observed in the CE associating with higher nutrients and Chl-*a* indicating higher primary production in the CE than ACE region (Fig. 4). In contrast, low PN and POC (Fig. 4a,b) in the ACE regions are associated with low nutrients (Fig. 3) and low Chl-*a* (Fig. 2c) indicating existence of oligotrophic conditions (Fig. 4). The mean C:N ratio of POM (10.6 ± 3.1) is higher than the typical Redfield ratio of 6.6 indicating possible modification of organic matter. Nevertheless, the mean C:N ratio does not indicate possible contribution of terrestrial organic matter (C:N >20; Kao and Liu 2000) in the study region suggesting that *in situ* processes may be contributed to the POM pool. The POC:Chl-*a* (wt:wt) is used as a proxy to identify source of organic matter in the aquatic environment (Cifuentes et al., 1988; Richard et al., 1997; Bentaleb et al., 1998). Typically POC:Chl-*a* ratio is low in the freshly produced organic matter compared to terrestrial organic matter. Wide range of POC:Chl-*a* ratios are proposed (40 to 200; Montagnes et al., 1994; Geider, 1987; Head et al., 1996; Thomson et al., 1992; Bentaleb et al., 1998) for *in situ* organic matter due to regional differences in temperature, light, phytoplankton composition and their growth rate (Heath et al., 1990; Geider et al., 1998). In addition to this, variable rate of decomposition of POC and Chl-*a* also governs POC:Chl-*a* ratio. The mean POC:Chl-*a* (1123 ± 389) in the BoB suggests 1) faster decomposition of Chl-*a* than POC, 2) possible contribution of heterotrophs (bacteria, zooplankton) and 3) contribution of terrestrial organic matter. The occurrence of terrestrial organic matter is possible as several rivers, such as Ganges, Godavari, Mahanadi etc., open to the BoB that may bring significant amount of organic matter to the BoB (Ittekkot et al., 1991; Unger et al., 2003). The river discharge peaks during monsoon (June to October) when high river-borne organic matter enters to the northern BoB. The sediment trap studies revealed that terrestrial POM is settled within 100 km from the coast (Ittekkot et al., 1991; Kumar et al., 2004; 2010). The strong linear relationship was observed between salinity and $\delta^{15}\text{N}_{\text{POM}}$ during September and October suggesting possible contribution of organic matter through river discharge (Kumar et al., 2004). Low saline (<32) waters were observed in the CE and ACE_N regions and it may be possible that river borne nutrients may support part of the primary production and therefore POM. Due to unavailability

of isotopic composition of nitrogen in nitrate or ammonium in the Ganges and Brahmaputra rivers, it is difficult to account possible contribution of riverine-nutrients and therefore POM production. Nevertheless, no significant relationship was observed between salinity and $\delta^{15}\text{N}_{\text{POM}}$ ($r^2=0.00$; Fig. 5) during present study indicating insignificant contribution of terrestrial organic matter may be possible in the study region. Added to this, the mean $\delta^{13}\text{C}_{\text{POM}}$ ($-24.4\pm 0.8\text{‰}$) is close to that of marine origin ($-23.2\pm 1\text{‰}$; Galvan et al., 2008) further indicate that insignificant contribution of terrestrial organic matter in the study region.

The origin of organic matter (marine versus terrestrial) can be identified using $\delta^{13}\text{C}_{\text{POM}}$ and $\delta^{15}\text{N}_{\text{POM}}$ (Kumar et al., 2004; Faganeli et al., 2009; Maya et al., 2011; Sarma et al., 2014; Krishna et al., 2014). Due to different fractionation associated with the inorganic carbon uptake of terrestrial and aquatic plants, the $\delta^{13}\text{C}_{\text{POM}}$ is variable. On the other hand, different isotopic composition of $\delta^{15}\text{N}$ of inorganic nitrogen from various sources, such as fertilizers, sewage, soil organic matter-derived, and their uptake by plankton store these signatures in their body (Thornton and McManus, 1994). Several observations suggested that lower isotopic composition of $\delta^{13}\text{C}$ for C_3 type (-30 to -25‰ ; Middelburg and Nieuwenhuize, 1998; Barth et al., 1998) whereas it is higher for C_4 type (-17 to -9‰ ; Smith and Epstein, 1971; Sackett, 1989). The $\delta^{13}\text{C}$ of marine phytoplankton falls between C_3 and C_4 plants (-24 to -18‰ ; Peters et al., 1978; Fry and Sherr, 1984; Middelburg and Nieuwenhuize, 1998; McMahon et al., 2013). Similarly, $\delta^{15}\text{N}$ of terrestrial plants is lower (1.8 to 3.0‰ ; Peters et al., 1978; Wada et al., 1987; Thornton and McManus, 1994) than marine phytoplankton (5 - 8‰ ; Altabet, 1996; Brandes and Devol, 2002; Lamb et al., 2006). The $\delta^{13}\text{C}_{\text{POM}}$ and $\delta^{15}\text{N}_{\text{POM}}$ in the BoB ranged from -27.2 to -19.7‰ and 2.1 to 8.6‰ respectively with relatively lower than expected from marine sources. The BoB receives significant amount of fresh water from the Ganges river that contains depleted $\delta^{13}\text{C}_{\text{DIC}}$ (-7.2‰ ; Samanta et al., 2015). The occurrence of low saline water in the upper 20-25m of water column can be observed in the study region, especially up to the distance of 1200 km. The mean $\delta^{13}\text{C}_{\text{DIC}}$ is $-2\pm 0.5\text{‰}$ in the mixed layer (Our unpublished data) suggesting assimilation of depleted DIC might have decreased $\delta^{13}\text{C}_{\text{POM}}$. Based on the SIAR model, the contribution of terrestrial and marine organic matter was estimated using $\delta^{13}\text{C}_{\text{POM}}$ and $\delta^{15}\text{N}_{\text{POM}}$ and isotopic composition of carbon and nitrogen of source organic matter and found that $\sim 10\%$ of the organic matter is contributed by detritus from C_3 and C_4 plants and $\sim 10\%$ by the soil organic matter and about 80% by the marine organic matter. Make a note that the uncertainties involved in these estimations are up to 15% . Based on C/N, POC/Chl-a, $\delta^{13}\text{C}_{\text{POM}}$, $\delta^{15}\text{N}_{\text{POM}}$ and isotopic mixing model, it is concluded that POM mainly derived from *in situ* processes during study period in the BoB.

Saino and Hattori (1980) suggested that the source of nitrogen in the euphotic zone is reflected in $\delta^{15}\text{N}_{\text{POM}}$. Though source of nutrients taken up by the phytoplankton may reflect in the $\delta^{15}\text{N}_{\text{POM}}$, trophic processes, however, modify its signatures. For example, microbial decomposition of organic matter increases $\delta^{13}\text{C}$ and $\delta^{15}\text{N}$ values as well as POC:PN ratio due to preferential decomposition of labile organic compounds (Hedges et al., 1997). Nevertheless, lower $\delta^{15}\text{N}_{\text{POM}}$ values ($2.8\pm 0.6\%$) were found associating with deeper nitracline (62 to 66 m) in ACEs whereas higher values ($5.2\pm 1\%$) were observed in the CE and NE regions coinciding with shallow nitracline (14 to 17 m). In case of deeper nitracline, the supply of new nitrogen from subsurface water may be almost negligible; hence, phytoplankton has to rely on regenerated nutrients, and excretory products of heterotrophs, which have low $\delta^{15}\text{N}$ values compared to their body (Checkley and Entzeroth, 1986; Checkley and Miller, 1986). Therefore, the assimilation of these nitrogenous nutrients decreases the $\delta^{15}\text{N}_{\text{POM}}$. The depleted $\delta^{15}\text{N}_{\text{POM}}$ values can also be attributed to nitrogen fixation, atmospheric deposition of nitrogen and uptake of dissolved organic nitrogen (DON).

In order to examine the possible nitrogen fixation, the spatial variations in N^* (an indicator of nitrogen fixation following Gruber and Sarmiento, 1997) was computed in the mixed layer. The positive N^* values (0.2 to 2.6 μM) were observed associated with low saline waters in the northern BoB (station 1 to 4; CE region) in the mixed layer and negative values were observed in the other study region. The occurrence of nitrogen fixers (*Trichodesmium*) was reported in the southern and southeastern BoB and it was not reported in the study region (i.e., western BoB) (Hegde et al., 2008). In addition to this, abundance of nitrogen fixers was not found in this study based on both microscopic and pigment analysis (Dr. J. Loganathan, personal communication, 2018). The mean value of $\delta^{15}\text{N}_{\text{POM}}$ in the CE region was $\sim 5.0\%$ which is close to that of deep water nitrate value ($\sim 5.5\%$; Bristow et al., 2017) suggesting new nitrate from the deep water supporting primary production. N^* technique was developed based on the global mean nitrate and phosphate data and may not be applicable to the region which receives high river discharge. Wide variations in N:P ratios were reported in the Indian river estuaries (Sarma et al., 2010) and about 10% of the estuarine nutrients are exported to the coastal waters in the BoB (Krishna et al., 2015). Since river water brings nutrients with different N:P ratios, the assumption of N:P of 16 in the equation of Gruber and Sarmiento (1997) to compute N^* may not be valid. Nevertheless, the negative N^* values are observed in both ACE_N and ACE_S where lower $\delta^{15}\text{N}_{\text{POM}}$ values were observed (4.0 ± 0.8 and $3.7\pm 0.7\%$ in the ACE_N and ACE_S respectively; Table 1), suggesting that processes other than nitrogen fixation may be responsible. Atmospheric dust deposition is also a possible source of nitrogen as BoB receives significant amount of atmospheric dust from Indo-Gangetic Plain during

the study period (Kumar et al., 2008; Srinivas and Kumar, 2013). Therefore, dry deposition of atmospheric nitrogen and its uptake by the phytoplankton would also deplete $\delta^{15}\text{N}_{\text{POM}}$ in the mixed layer.

TSP in the atmosphere ranged between 9.6 and 20.6 $\mu\text{g m}^{-3}$ along the cruise track and concentration of nitrate in the atmospheric dust varied from 0.08 to 0.28 $\mu\text{gN m}^{-3}$. The flux of nitrate was calculated using the following equation (Duce et al., 1991):

$$\text{Dry-Depositon flux (f}_{\text{dry}}) = C_{\text{measured}} \times V_{\text{dry}}$$

Where C_{measured} is the concentration of nitrate in the aerosols and V_{dry} is the dry deposition velocity. V_{dry} for nitrate was taken as 1.0 cm sec^{-1} (Duce et al., 1991; Srinivas et al., 2013).

Nitrate dry-deposition flux ranged between 68.8 and 240.6 $\mu\text{gN m}^{-2} \text{d}^{-1}$ in the study region. Assuming the all the deposited nitrate is utilized by the phytoplankton and using C/N ratio of 6.6, the atmospheric deposition may increase primary production by 0.45 to 1.58 $\text{mgC m}^{-2} \text{d}^{-1}$. The primary production in the mixed layer was ranged from 80 to 420 $\text{mgC m}^{-2} \text{d}^{-1}$ (Dr. H.B. Delabehera, personal communication, 2018). Therefore, the atmospheric deposition enhanced primary production up to 1% in the mixed layer. However, the contribution of atmospheric nitrogen may be higher during winter when the atmospheric aerosol loading is several times higher (Srinivas et al., 2011; Yadav et al., 2016). On the other hand, uptake of DON, as an alternative source of nitrogen, is also possible for depleted $\delta^{15}\text{N}_{\text{POM}}$ in the BoB. Prasad (2014) observed DON concentrations in the range of 5 to 15 μM in the coastal BoB during monsoon period. The uptake of DON by phytoplankton, in the absence or lower concentrations of inorganic nitrogen, results in lower $\delta^{15}\text{N}_{\text{POM}}$ (Saino and Hattori, 1980). Neither concentration of DON nor their isotopic composition is available during study period to evaluate its impact. Relatively higher ammonium concentrations in the ACE ($>1 \mu\text{M}$) regions suggest that regenerated nutrients may be possible source of nutrients. The mean $\delta^{15}\text{N}_{\text{POM}}$ values in the ACE_N and ACE_S were relatively lower (4.0 ± 0.8 and $3.7 \pm 0.7\text{‰}$ respectively) than CE and NE regions (5.0 ± 0.6 and $4.8 \pm 0.7\text{‰}$ respectively; $t_{\text{stat}} = -1.05$; $p < 0.1$) suggesting uptake of regenerated nutrients may be possible in the ACEs. Isotopic studies, such as triple oxygen isotopes of oxygen in nitrate and nitrogen isotopic composition of DON, are required to confirm the contribution of various source of nitrogen supporting phytoplankton biomass in the BoB. The mean values of $\delta^{15}\text{N}_{\text{POM}}$ in the CE and NE regions ($\sim 5.0\text{‰}$) is close to that of deeper water nitrate value of 5.5‰ (Bristow et al., 2017) further suggesting that new nitrogen from subsurface waters supported phytoplankton production in CE region.

4.2. Influence of eddies on f-ratios in the BoB

The nitracline depth displayed significant inverse relation with $\delta^{15}\text{N}_{\text{POM}}$ in the mixed layer ($r^2=0.55$; $p<0.001$; Fig. 6) suggesting that the availability of subsurface nitrate controlled the phytoplankton production in the BoB. The depth of nitracline showed significant inverse relation with POC ($r^2=0.35$; $p<0.05$) and PN ($r^2=0.32$; $p<0.05$) suggesting that phytoplankton production in the mixed layer is controlled by depth of nitracline. Mino et al. (2002) suggested that the source of nitrogen is reflected in the $\delta^{15}\text{N}_{\text{POM}}$ in the mixed layer. Recently Sherin et al. (2018) also showed significant variations in $\delta^{15}\text{N}_{\text{POM}}$ in the CE and cyclone-influenced regions in the BoB during November-December 2013 and suggested that nitrate from deep water supported primary production in the CE and cyclone-influenced region and regenerated nitrate in the other regions. Interestingly the slope of relationship between nitracline depth and $\delta^{15}\text{N}_{\text{POM}}$ is similar with reference to space (0.047 in Atlantic Ocean; Mino et al., 2002 and 0.041 in BoB; Sherin et al., 2018). This slope is same with reference to time as it was 0.041 during November-December 2013 (Sherin et al., 2018) and March-April 2018 (0.043; present study) in the BoB. Similarly, the intercept of the relation is also insignificantly different in the Atlantic Ocean (5.7; Mino et al., 2002), BoB (6.3; Sherin et al., 2018) and present study (5.6). The uniform slope and intercept in different basins and different periods strongly indicate the robustness of the relationship, which is mainly caused by uniform deep water $\delta^{15}\text{N}_{\text{NO}_3}$ (Sigman et al., 1997). This relationship suggests that shallow nitracline enhances input of nitrate from the subsurface waters with relatively higher $\delta^{15}\text{N}$ (5-6‰) leading to enrichment of $\delta^{15}\text{N}$ of phytoplankton and contrasting to that occurs in deeper nitracline regions where regenerated nitrogen, and DON uptake may support phytoplankton production leading to low $\delta^{15}\text{N}_{\text{POM}}$. However, the relationship between $\delta^{15}\text{N}_{\text{sus}}$ and depth of nitracline may be different during monsoon period when high amount of terrestrial organic matter is injected through river discharge.

Based on Mino et al. (2002), assuming phytoplankton are supported by nutrients from deep water and regenerated nutrients, the $\delta^{15}\text{N}$ of plankton can be estimated using following equation:

$$\delta^{15}\text{N}_{\text{plankton}} = f_{\text{new:N}} \times \delta^{15}\text{N}_{\text{newN}} + (1-f_{\text{new:N}}) \times \delta^{15}\text{N}_{\text{regen N}} \quad (2)$$

Where $f_{\text{new:N}}$ (dimensionless) is the fraction of new nitrate supported to total primary production, and $\delta^{15}\text{N}_{\text{plankton}}$, $\delta^{15}\text{N}_{\text{newN}}$ and $\delta^{15}\text{N}_{\text{regenN}}$ are the isotopic compositions of plankton, new nitrate and regenerated nitrogen respectively (Mino et al., 2002). Here f_{newN} and $\delta^{15}\text{N}_{\text{regenN}}$ are estimated from their relationship with depth of nitracline (D_{NO_3}) following Mino et al. (2002).

$$f_{\text{newN}} = A/D_{\text{NO}_3} \quad (3)$$

$$\delta^{15}\text{N}_{\text{regN}} = \delta^{15}\text{N}_{\text{newN}} - B \times D_{\text{NO}_3} \quad (4)$$

where A and B are proportionality constants. The final relation shown below is obtained by combining all the above three equations

$$\delta^{15}\text{N}_{\text{plankton}} = -B \times D_{\text{NO}_3} + (\delta^{15}\text{N}_{\text{newN}} + A \times B) \quad (5)$$

Since POM is mainly derived from *in situ* production, here $\delta^{15}\text{N}_{\text{POM}}$ is equal to $\delta^{15}\text{N}_{\text{plankton}}$. The mean $\delta^{15}\text{N}_{\text{NO}_3}$ in the northern BoB (5.5‰; Bristow et al., 2017) is assumed to be same in the entire BoB as no denitrification occurs in the Bay (Sarma et al., 2016 and references therein). The values for A and B are calculated as 8.475 m^{-1} and 0.043‰ respectively and the former is used to calculate *f*-ratios from equation (3).

The estimated *f*-ratios varied between 0.11 and 0.34 in the BoB during study period with the average value of 0.23 ± 0.08 in the mixed layer. Relatively lower *f*-ratios were observed in the ACE_N (0.19 ± 0.09) and ACE_S (0.19 ± 0.06) than CE (0.31 ± 0.04) and NE (0.28 ± 0.05) in the BoB. The higher *f*-ratios in the CE region are associated with higher nitrate ($1.98 \pm 0.8 \mu\text{M}$) and Chl-*a* ($0.35 \pm 0.17 \text{ mg m}^{-3}$) than ACE_N ($0.02 \pm 0.05 \mu\text{M}$ and $0.11 \pm 0.04 \text{ mg m}^{-3}$ respectively) and ACE_S ($0.10 \pm 0.04 \mu\text{M}$ and $0.12 \pm 0.2 \text{ mg m}^{-3}$ respectively). These estimates of *f*-ratios are lower than earlier estimations using tracer incubation experiments (0.54-0.70; Kumar and Ramesh, 2005; Gandhi et al., 2010). Anand et al. (2018) observed low primary (15.2 and 74.1 $\text{mmol C m}^{-2} \text{ d}^{-1}$ in the ACE and NE regions respectively) and export production (0.6 and 1.3 $\text{mmol C m}^{-2} \text{ d}^{-1}$ respectively) in the BoB associated with ACE and it is consistent with the present study. Our study suggests that higher fraction of primary production is exported to depth below mixed layer in the CE region compared to ACE regions. The atmospheric deposition is estimated to contribute to 1% of primary production in the mixed layer. Similarly, the estimated *f*-ratio due to new production from atmospheric deposition is amounted to range from 0.003 to 0.005. Though atmospheric deposition may be adding some amount of nitrate however, its influence on primary production and *f*-ratio may be negligible during study period. Therefore, phytoplankton in the study region may be dominantly supported by new nitrogen from subsurface and regenerated nutrients during study period. This limitation of this method is that it gives mean *f*-ratios in the mixed layer. The mean MLD in the study region is 30 ± 5 m whereas depth of euphotic zone is 46 ± 6 m and it was observed that ~80% of the primary production in the euphotic zone occurs within 30m of the water column due to decrease in photosynthetic active radiation. Therefore, the estimated *f*-ratios may reflect variations in the euphotic zone.

Relatively lower dissolved oxygen is observed in the subsurface waters (depth below 75m) in the CE region ($\sim 60 \mu\text{M}$) compared to ACEs ($>150 \mu\text{M}$). Such low concentrations were mainly resulted from upward pumping of low oxygen waters from the subsurface layers. It is further noticed that CEs are important in promoting new production that may lead to long-term sustenance of the oxygen minimum zone (OMZ) in the BoB. In contrast, ACEs weaken OMZ due to ventilation of oxygen due to convergence (Sarma et al., 2013; 2016; 2018; Sarma and Uday Bhaskar, 2018). However, contribution of strong OMZ in the CE regions due to physical mixing and oxygen removal through microbial decomposition of organic matter must be evaluated. Several studies indicated that about 50 eddies forms every year in the BoB (Chen et al., 2012; Dandapath and Chakraborty, 2016) and it may have significant impact on photic zone production and OMZ and it may have ultimate impact on carbon sequestration and air-sea fluxes of CO_2 to the atmosphere. More intensive studies are required to examine the influence of eddies in the basin-wide primary and export production in the BoB.

Summary and conclusions

The content and isotopic composition of carbon and nitrogen of suspended particulate organic matter (POM) was sampled in the upper 100 m of water column along with hydrographic properties to examine the variation in source of organic matter, nutrients and f -ratios in the cyclonic (CE) and anticyclonic eddies (ACE) in the Bay of Bengal (BoB). Enhanced Chl- a , particulate organic carbon (POC) and nitrogen (PN) were observed associated with increase in nutrients in the CE and no-eddy (NE) regions compared to ACEs. This suggests that divergence of waters in the CE brought nutrients to surface that enhanced biological production. Based on variations in the C:N, POC:Chl- a , isotopic composition of carbon, and isotope mixing model, it is concluded that the POM mainly produced through *in situ* plankton production in the study region and contribution from terrestrial sources are negligible. The depth of nitracline displayed significant inverse relation with $\delta^{15}\text{N}_{\text{POM}}$ with relatively lower $\delta^{15}\text{N}_{\text{POM}}$ in the ACE than CE suggesting that subsurface nutrients supported phytoplankton production in the CE and regenerated and dissolved organic nitrogen in the ACE region. The estimated f -ratios were almost double in the CE (0.31) and NE (0.28) than ACEs (0.19) in the BoB suggesting that higher fraction of primary production is exported to the deeper depths in the CEs than ACEs. The higher POC and f -ratios in the CEs suggest further decrease in DO concentrations below 75m depth, apart from decrease in DO by physical mixing. However the contribution of decrease in DO due to enhanced production should be quantified. In contrast convergence of surface waters injected DO to the OMZ, in addition to this, less organic matter is exported to deeper depth leading to weaker OMZ in the ACE regions. More than 50 eddies (both ACE and CEs) form every year and they may significantly influence primary production, export of organic matter and intensity of OMZ

in the BoB. More studies are required involving moorings, bioargos and modeling efforts to understand the influence of eddies on carbon export to the meso-pelagic depths and variations in OMZ in the BoB.

Acknowledgements: We would like to thank the Director, CSIR-NIO and the Scientist-In-Charge, CSIR-NIO Regional Centre for their encouragement, support and allotment of ship time. We would like to thank Dr. Aparna, NIO and Mr. Sateesh, INCOIS for their help in sending SSHA daily maps to on board to guide us the course of our vessel. We would like to thank Editor, Associate Editor and three anonymous reviewers for their suggestions and comments to improve the presentation of our work. We would like to thank ESSO-INCOIS for funding this project. This has NIO contribution number....

References

Altabet, M.A. 1988., Variations in nitrogen isotopic composition between sinking and suspended particles: Implications for nitrogen cycling and particle transformation in the open ocean. *Deep-Sea Res*, I, 35, 535–554.

Altabet, M.A. 1996., Nitrogen and carbon isotopic tracers of the source and transformation of particles in the deep sea. In: Ittekkot V., Schaefer P., Honjo S. and Depetris P. J. (ed) *Particle flux in the Ocean*. SCOPE, Vol, 57, Wiley & Sons, Chichester, pp. 155-184.

Anand, S., Rengarajan, R., and Sarma, V.V.S.S., 2018. ^{234}Th based carbon export flux along the Indian GEOTRACES GI02 section in the Arabian Sea and the Indian Ocean. *Global Biogeochem. Cycles*, in press.

Aumont, O., Hulthen, M.V., Roy-Barman, M., Dutay, J.C.m, Ethe, Christian, and Gehlen, M. 2017., Variable reactivity of particulate organic matter in a global ocean biogeochemical model, *Biogeosci.*, 14, 2321-2341.

Barth, J.A.C., Veizer, J., and Mayer, B., 1998. Origin of particulate organic carbon in the upper St. Lawrence: Isotopic constraints. *Earth Plant. Sci. Lettrs*, 162, 111- 121.

Bentaleb, I., Fontugne, M., Descolas-Gros, C., Girardin, C., Mariotti, A., Pierre, C., et al. 1998. Carbon isotopic fractionation by plankton in the southern Indian Ocean: Relation between $\delta^{13}\text{C}$ of particulate organic carbon and dissolved carbon dioxide. *J. Mar. Syst.*, 17, 39–58. [https://doi.org/10.1016/S0924-7963\(98\)00028-1](https://doi.org/10.1016/S0924-7963(98)00028-1).

Brandes, J.A. and Devol, A.H., 2002. A global marine-fixed nitrogen isotopic budget: implications for Holocene nitrogen cycling. *Global Biogeochem. Cycles*, doi: 10.1029/2001GB001856.

Bristow, L.A., Callbeck, C.M., Larsen, M., Altabet, M.A., Dekaezemacker, J., Forth, M., Gauns, M., Glud, R.N., Kuypers, M.M.M., Lavik, G., Milucka, J., Naqvi, S.W.A., Pratihary, A., Revsbech, N.P., Thamdrup, B., Treusch, A.H., and Canfield, D.E., 2017. N_2 production rates

limited by nitrite availability in the Bay of Bengal oxygen minimum zone, *Nature Geosci.*, doi: 10.1038/NGEO2847.

Bunn, S.E., Longergan, N.R., Kempster, M.A., 1995. Effects of acid washing samples on stable isotope ratios of C and N in penaeid shrimps and seagrass: implications for food web studies using stable isotopes. *Limnol. Oceanogr.*, 40, 622-625.

Carritt, D.E., Carpenter, J.H. 1966. Comparison and evaluation of currently employed modifications of winkler method for determining dissolved oxygen in seawater – A Nasco report. *J Mar Res* 24,286–318.

Checkley, D.M. and Miller C.A., 1986. Nitrogen isotopic fractionation by oceanic zooplankton. *Eos Trans. AGU* 67, 988.

Checkley, D.M., Entzeroth L.C., 1985. Elemental and isotopic fractionation of carbon and nitrogen by marine, planktonic copepods and implications to the marine nitrogen cycle. *J. Plank. Res.*, 7, 553-568.

Chen, G., Wang, D., Hou, Y., 2012. The features and interannual variability mechanism of mesoscale eddies in the Bay of Bengal. *Cont. Shelf Res.*, 47, 178-185.

Chelton, D.B., Schlax, M.G., and Samelson, R.M. 2011. Global observations of nonlinear mesoscale eddies. *Prog. Oceanogr.*, 91, 167-216.

Cifuentes, L. A., Sharp, J. H., and Fogel, M. L., 1988. Stable carbon and nitrogen isotope biogeochemistry in the Delaware estuary. *Limnol. Oceanogr.*, 33, 1102–1115.

Dandapath, S. and Chakraborty, A., 2016. Mesoscale eddies in the Weestern Bay of Bengal as observed from satellite altimetry in 1993-2014: Statistical characteristics, variability and three-dimensional properties. *IEEE J. Appl. Earth Obser. Remote Sens.*, doi: 10.1109/JSTARS.2016.2585179.

Denman, K.L. and Abbott, M.R., 1994. Timescales of pattern evolution from cross-spectrum analysis of advanced very high resolution radiometer and coastal zone color scanner imagery. *J. Geophys. Res.* 99, 7433-7442.

Dickson, M.L., Orchardo, J., Barber, R.T., Marra, J., McCarthy, J.J., Sambrotto, R.N., 2001, Production and respiration rates in the Arabian Sea during the 1995 northeast and southwest monsoons, *Deep Sea Res., Part II*, 48, 1199–1230.

Doblin, M.A., Petrou, K., Sinutok, S., Seymour, J.R., Messer, L.F., Brown, M.V., Norman, L., Everett, J.D., McInnes, A.S., Ralph, P.J., Thompson, P.A., and Hassler, C.S. 2016. Nutrient uplift in a cyclonic eddy increases diversity, primary productivity and iron demand of microbial communities relative to a western boundary current. *PeerJ.*, 4: e1973, doi: 10.7717/peerj.1973.

- Duarte, C.M., Regaudie-de-Gioux, A., Arrieta, J.M., Delgado-Huertas, A., Agusti, S., 2013. The oligotrophic ocean is heterotrophic, *Annu. Rev. Mar. Sci.*, 5, 551-569.
- Duce, R.A., Liss, P.S., Merrill, J.T., Atlas, E.L., Buat-Menard, P., Hicks, B.B., Miller, J.M., Prospero, J.M., Arimoto, R., Church, T.M., Ellis, W., Galloway, J.N., Hansen, L., Jickells, T.D. et al. 1991. The atmospheric input of trace species to the world ocean, *Global Biogeochem. Cycles.*, 5, 193-258.
- Faganeli, J., Ogrinc, N., Kovac, N., Kukovec, K., Falnoga, I., Mozetic, P. and Bajt, O., 2009. Carbon and nitrogen isotope composition of particulate organic matter in relation to mucilage formation in the northern Adriatic Sea. *Mar. Chem.*, 114, 102-109.
- Fry, B. and Sherr, E., 1984. $\delta^{13}\text{C}$ measurements as indicators of carbon flow in marine and freshwater ecosystems. *Cont. Mar. Sci.*, 27, 13-47.
- Galvan, K, Fleeger J.W. and Fry, B. 2008. Stable isotope addition reveals dietary importance of phytoplankton and microphytobenthos to salt marsh infauna. *Mar. Ecol. Prog. Ser.*, 359, 27-49
- Gandhi, N., Prakash, S., Ramesh, R., Kumar, S., 2010a. Nitrogen uptake rates and new production in the northern Indian Ocean. *Indian J Mar. Sci.*, 39, 362-368.
- Gaube, P., McGillicuddy Jr, D.J., Chelton, D.B., Behrenfeld, M.J., Strutton, P.G. 2014. Regional variations in the influence of mesoscale eddies on near-surface chlorophyll. *J. Geophys. Res., Oceans*: 119, 8195-8220.
- Gauns, M., Madhupratap, M., Ramaiah, N., Jyothibabu, R., Fernandes, V., Paul, J.T., Prasanna Kumar, S., 2005. Comparative accounts of biological productivity characteristics and estimates of carbon fluxes in the Arabian Sea and Bay of Bengal. *Deep-Sea Res., II* 52, 2003-2017.
- Geider, R.J. 1987. Light and temperature dependence of the carbon to chlorophyll-a ratio in microalgae and cyanobacteria: implications for physiology and growth of phytoplankton, *New Phytologist*, 106, 1-34.
- Goering, J., Alexander, V., Haubensack, N., 1990. Seasonal variability of stable carbon and nitrogen isotope ratios of organisms in a north pacific bay. *Estuar. Coastal and Shelf Sci.* 30, 239-260.
- Grasshoff, K., Ehrhardt, M., Kremling, K., (Eds.) 1983. *Methods of Seawater Analysis*, Verlag Chemie, Weinheim, pp. 89-224.
- Gruber, N and J.L. Sarmiento, 1997. Global patterns of marine nitrogen fixation and denitrification, *Global Biogeochem. Cycles*, 11, 235-266.
- Head, E.J.H., Harrison, W.G., Irwin, B.I., Horne, E., Li, W.K.W., 1996. Plankton dynamics and carbon flux in an area of upwelling off the coast of Morocco. *Deep-Sea Res., I*, 43, 1713- 1738.
- Heath, M. R., Richardson, K., and Kiørboe, T., 1990. Optical assessment of phytoplankton nutrient depletion. *J. Plank. Res.*, 12, 381-396. <https://doi.org/10.1093/plankt/12.2.381>.

Hedges, J.I., Keil, R.G., Benner R., 1997. What happens to terrestrial organic matter in the ocean?. *Organic Geochem.*, 27, 195-212.

Hegde, A., Anil, A.C., Patil, J.S., Mitbavkar, S., Krishnamurthy, V., and Gopalakrishna, V.V. 2008. Influence of environmental settings on the prevalence of *Trichodesmium* spp. In the Bay of Bengal. *Mar. Ecol. Progr. Ser.*, 356, 93-101.

Ittekkot, V., Nair, R.R., Honjo, S., Ramaswamy, V., Bartsch, M., Manginini, S., Desai, B.N., 1991. Enhanced particle fluxes in Bay of Bengal induced by injection of fresh water. *Nature* 351, 385–387.

Kao, S.J., Liu, K.K. 2000. Stable carbon and nitrogen isotope systematic in a human disturbed watershed (Lanyang-His) in Taiwan and the estimation of biogenic particulate organic carbon and nitrogen fluxes. *Global Biogeochem. Cycles*, 14,189–198

Krishna, M.S., Naidu, S.A., Subbaiah, Ch.V., Gawade, L., Sarma, V.V.S.S., Reddy, N.P.C. 2014. Sources, distribution and preservation of organic matter in a tropical estuary (Godavari, India), *Estuaries and Coasts*, doi: 10.1007/s12237-014-9859-5.

Krishna, M.S., Prasad, M.H.K., Rao, D.B., Viswanadham, R., Sarma, V.V.S.S., Reddy, N.P.C., 2016. Export of dissolved inorganic nutrients to the northern Indian Ocean from the Indian monsoonal rivers during discharge period. *Geochem. Cosmochem. Acta*, 172-430-443.

Kumar, S., Ramesh, R., 2005. Productivity measurements in the Bay of Bengal using ¹⁵N tracer: Implications to the global carbon cycle. *Indian J Mar. Sci.*, 34, 153-162.

Kumar, S., Ramesh, R., Bhosle, N.B., Sardesai, S., Sheshshayee, M.S., 2004. Natural isotopic composition of nitrogen in suspended particulate matter in the Bay of Bengal. *Biogeosci.* 1, 63-70.

Kumar, A., Sudheer, A. K. and Sarin, M. M. 2008. Chemical characteristics of aerosols in MABL of Bay of Bengal and Arabian Sea during spring inter-monsoon: a comparative study. *J. Earth Syst. Sci.*, 117, 325_332.

Kumar, S., Ramesh, R., Dwivedi, R.M., Raman, M., Sheshshayee, M.S., D'Souza, W., 2010. Nitrogen uptake in the northeastern Arabian Sea during winter cooling. *International J Oceanogra.*, 819029.

Lamb, A.L., Wilson, G.P. and Leng, M.J., 2006. A review of coastal palaeoclimate and relative sea-level reconstructions using $\delta^{13}\text{C}$ and C/N ratios in organic material. *Earth Sci. Rev.*, 75, 29-57.

Levy, M., Memery, L., and Madec, G. 1998. The onset of a bloom after deep winter convection in the northwest Mediterranean Sea: mesoscale process study with a primitive equation model. *J. Mar. Sys.*, 16, 7-21.

Madhupratap, M., Gauns, M., Ramaiah, N., Prasanna Kumar, S., Muraleedharan, P.M., De Sousa, S.N., Sardesai, S., Muraleedharan, U., 2003. Biogeochemistry of the Bay of Bengal:

physical, chemical and primary productivity characteristics of the central and western Bay of Bengal during summer monsoon 2001. *Deep-Sea Res, II* 50, 881-896.

Mahadevan, A., and Archer, D. 2000. Modeling the impact of fronts and mesoscale circulation on the nutrient supply and biogeochemistry of the upper ocean. *J. Geophys. Res.*, 105, 1209-1225.

Maya, M.V., Karapurkar S.G., Naik, H., Roy, R., Shenoy, D.M. and Naqvi, S.W.A., 2011. Intra-annual variability of carbon and nitrogen stable isotopes in suspended organic matter in waters of the western continental shelf of India. *Biogeosci.*, 8, 3441-3456.

McCarthy, J.J., Garside, C., John L.N., 1999. Nitrogen dynamics during the Arabian Sea northeast monsoon. *Deep-Sea Res, II* 46, 1623-1664.

McGillicuddy, Jr., D.J., Anderson, L.A., Doney, S.C., and Maltrud, M.E. 2003. Eddy-driven sources and sinks of nutrients in the upper ocean: Results from a 0.1o resolution model of the North Atlantic. *Global Biogeochem. Cycles.*, 17, 1035, doi: 10.1029/2002GB001987.

McGillicuddy, Jr. D.J., 2016. Mechanisms of physical-biological-biogeochemical interaction at the oceanic mesoscale. *Ann. Rev. Mar. Sci.*, 8, 13.1-13.36, doi: 10.1146/annurev-marine-010814-015606.

McMahon, K.W., Ling Hamaday, L. and Thorrold, S. R., 2013. A review of ecogeochemistry approaches to estimating movements of marine animals. *Limnol. Oceanogr.*, 58, 697–714.

Middelburg, J.J., Nieuwenhuize, J., 1998. Carbon and nitrogen stable isotopes in suspended matter and sediments from the Schelde Estuary. *Mar. Chem.*, 60, 217-225.

Mino, Y., Saino, T., Suzuki, K., Maranon, E., 2002. Isotopic composition of suspended particulate nitrogen ($\delta^{15}\text{N}_{\text{sus}}$) in surface waters of the Atlantic Ocean from 50° N to 50° S. *Global Biogeochem. Cycles* 16, 1059.

Montagnes, D. J. S., Berges, J. A., Harrison, P. J., and Taylor, F. J. R., 1994. Estimating carbon, nitrogen, protein and chlorophyll a from volume in marine phytoplankton. *Limnol. Oceanogr.*, 39, 1044–1060. <https://doi.org/10.4319/lo.1994.39.5.1044>.

Nagai, T., Gruber, N., Frenzel, H., Lachkar, Z., McWilliams, J.C., and Plattner, G.K. 2015. Dominant role of eddies and filaments in the offshore transport of carbon and nutrients in the California Current System. *J. Geophys. Res. Oceans*, 120, 5318-5341, doi: 10.1002/2015JC010889.

Oschlies, A., and Garcon, V. 1998. Eddy-induced enhancement of primary production in a model of the North Atlantic Ocean. *Nature*, 394, 266-269.

Parnell, A., Inger, R., Bearhop, S., and Jackson, A.L. 2010. Source partitioning using stable isotopes coping with too much variation. *Plos One*, 5, 9672.

Peters, K.E., Sweeney, R.E. and Kaplan, I.R., 1978. Correlation of carbon and nitrogen stable isotope ratios in sedimentary organic matter. *Limnol. Oceanogr.*, 23, 598-604.

Pinnegar, J.K., Polunin, N.V.C., 1999. Differential fractionation of $\delta^{13}\text{C}$ and $\delta^{15}\text{N}$ among fish tissues: implications for the study of trophic interactions. *Functional Ecology* 13, 225-231.

Prasanna Kumar, S., Nuncio, M., Narvekar, J., Kumar, A., Sardesai, S., De Souza, S.N., Gauns, M., Ramaiah, N., Madhupratap, M., 2004. Are Eddies nature's trigger to enhance biological productivity in the Bay of Bengal?. *Geophys. Res. Lett.*, 31, L07309.

Sackett, W. M. 1989, Stable carbon isotope studies on organic matter in the marine environment, in *Handbook of Environmental Isotope Geochemistry*, edited by P. Fritz and J. C. Fontes, pp. 139–169, Elsevier, New York.

Saino, T. and Hattori, A., 1980. ^{15}N natural abundance in oceanic suspended particulate matter. *Nature*, 283, 752-754.

Samanta, S., T.K. Dalai, J.K. Pattanaik, S.K. Rai and A. Mazumdar., 2015. Dissolved inorganic carbon (DIC) and its $\delta^{13}\text{C}$ in the Ganga (Hooghly) river estuary, India: Evidence of DIC generation via organic carbon degradation and carbonate dissolution. *Geochim. Cosmochim. Acta*, 165, 226-248.

Sarma, V.V.S.S., Krishna, M.S., Viswanadham, R., Rao, G.D., Rao, V.D., Sridevi, B., Kumar, B.S.K., Prasad, V.R., Subbaiah, Ch.V., Acharyya, T., and Bandopadhyay, D., 2013. Intensified oxygen minimum zone on the western shelf of Bay of Bengal during summer monsoon: Influence of river discharge, *J. Oceanogr.*, 69, 45-55.

Sarma, V.V.S.S., Kumar, M.D., and Saino, T., 2006. Impact of sinking carbon flux on accumulation of deep-ocean carbon in the Northern Indian Ocean. *Biogeochem.*, doi: 10.1007/s10533-006-9055-1.

Sarma, V.V.S.S., 2009. Net Community Production in the northern Indian Ocean, In: *Indian Ocean biogeochemical processes and ecological variability*, American Geophysical Union, Washington DC, USA, 239-256.

Sarma, V.V.S.S., Prasad, V.R., Kumar, B.S.K., Rajeev, K., Devi, B.M.M., Reddy, N.P.C.,

Sarma, V.V., Kumar, M.D. 2010. Intra-annual variability in nutrients in the Godavari estuary. *India. Cont Shelf Res* 30:2005–2014

Sarma, V.V.S.S., Rao, G.D., Viswanadham, R., Sherin, C.K., Salisbury, J., Omand, M.M. Mahadevan, A., Murty, V.S.N., Shroyer, E.L., Baumgartner, M., Stafford, K., 2016. Effects of freshwater stratification on nutrients, dissolved oxygen and phytoplankton in the Bay of Bengal. *Oceanography*, 29, 126-135.

Sherin, C.K., Sarma, V.V.S.S., Rao, G.D., Viswanadham, R., Omand, M.M. and Murty, V.S.N., 2018. New to total primary production ratio (f-ratio) in the Bay of Bengal using isotopic composition of suspended particulate organic carbon and nitrogen. *Deep Sea Research Part I: Oceanographic Research Papers*.

Sigman, D.M., Altabet, M.A., Michener, R., McCorkle, D.C., Fry, B., Holmes, R.M., 1997. Natural abundance-level measurement of the nitrogen isotopic composition of oceanic nitrate: An adaptation of the ammonia diffusion method. *Mar. Chem.*, 57, 227-242.

Smith, B.N. and Epstein, S., 1971. Two categories of $^{13}\text{C}/^{12}\text{C}$ ratios for higher plants. *Plant Physiology (Bethesda)* 47, 380-384.

Smith, B.N. and Epstein, S., 1971. Two categories of $^{13}\text{C}/^{12}\text{C}$ ratios for higher plants. *Plant Physiology (Bethesda)* 47, 380-384.

Srinivas, B. and Sarin, M. M. 2013. Atmospheric deposition of N,P and Fe to the Northern Indian Ocean: implications to C- and N-fixation. *Sci. Total Environ.*, 456-457, 104-114.

Strass, V. 1992. Chlorophyll patchiness caused by mesoscale upwelling at fronts. *Deep-Sea Res.*, 39, 75-96.

Srinivas, B., Sarin, M.M. and Sarma, V.V.S.S. 2011. Atmospheric dry deposition of inorganic and organic nitrogen to the Bay of Bengal: Impact of continental outflow. *Mar. Chem.*, 127, 170-179.

Suzuki R, and Ishimaru, T, 1990. An improved method for the determination of phytoplankton chlorophyll using N,N-dimethylformamide. *J Oceanogr.*, 46, 190–194

Thompson, P.A., Guo, M., Harrison, P.J.,1992. Effects of variation in temperature. I. On the biogeochemical composition of eight species of marine phytoplankton, *J. Phycology*, 28, 481-488.

Unger, D., Ittekkot, V., Schafer, P., Tiemann, J., and Reschke, S., 2003. Seasonality and interannual variability of particle fluxes to the deep Bay of Bengal: Influence of riverine input and oceanographic processes, *Deep Sea Res., Part II*, 50, 897–923.

Vidya, P.J., Prasanna Kumar, S., 2013. Role of mesoscale eddies on the variability of biogenic flux in the northern and central Bay of Bengal. *J. Geophys. Res., Oceans* 118, 5760- 5771.

Wada E., Minagawa M., Mizutani H., Tsuji T., Imaizumi R. and Karasawa K., 1987. Biogeochemical studies on the transport of OM along the Otsuchi River watershed, Japan. *Estuarine Coastal Shelf Sci.*, 25, 321–336.

Yadav, K., Sarma, V.V.S.S., Rao, D.B., and Kumar, M.D. 2016. Influence of atmospheric dry deposition of inorganic nutrients on phytoplankton biomass in the coastal Bay of Bengal. *Mar. Chem.*, 187, 25-34.

Table 1: Mixed layer mean variation along with standard deviations in biogeochemical properties in various eddies in the BoB are given. DNO_3 is depth of nitracline (m).

Parameter	CE	ACE _N	NE	ACE _S	CE vs ACE T _{stat} & p-value
Chl- <i>a</i> (mg m ⁻³)	0.35±0.17	0.11±0.04	0.22±0.12	0.10±0.04	1.71; <0.05
NO ₃ (μM)	1.98±2	0.02±0.05	1.58±1.5	0.12±0.2	3.36; <0.001
DNO ₃ (m)	14±2	62±5	17±2	66±4	-5.62; <0.001
TSM (mg l ⁻¹)	5.6±0.9	4.3±0.6	4.0±0.8	4.1±0.6	2.90; <0.001
PN (μg l ⁻¹)	22.5±2	6.9±2	14.0±1	8.5±3	8.74; <0.001
POC (μg l ⁻¹)	158.5±10	92.4±9	132.0±3	88.1±8	3.13; <0.001
C/N	8.6±2	17.2±4	8.0±2	10.8±3	-4.75; <0.001
δ ¹⁵ N _{POM} (‰)	5.0±0.6	4.0±0.8	4.8±0.7	3.7±0.7	-1.05; <0.1
δ ¹³ C _{POM} (‰)	-25.3±0.6	-24.2±0.7	-23.8±1	-23.4±1	-3.78; <0.001
<i>f</i> -ratio	0.31±0.04	0.19±0.09	0.28±0.05	0.19±0.06	-1.06; <0.01

Legend to figures

Figure 1: The study region with station locations. The color back ground shows the variations in SSHA. Direction and speed of surface water geostrophic currents are shown as arrows. Only nitrate and ammonium data were collected at station A.

Figure 2: Vertical distribution of a) temperature ($^{\circ}\text{C}$), b) Salinity, c) Chlorophyll-a (mg m^{-3}) and d) DO (μM) in the color scale along the cruise track in the BoB. The density contours are given in all maps. Station numbers and stations considered under CE, ACE_N, ACE_S and NE regions were also shown. The depth of mixed layer is shown as white line.

Figure 3: Vertical distribution of a) nitrate (μM), and b) ammonium (μM) along the cruise track in the BoB. Station numbers and stations considered under CE, ACE_N, ACE_S and NE regions were also shown.

Figure 4: Vertical distribution of a) POC ($\mu\text{g/l}$), b) PN ($\mu\text{g/l}$) c) $\delta^{13}\text{C}_{\text{POM}}$ and d) $\delta^{15}\text{N}_{\text{POM}}$ along the cruise track. The stations considered under CE, ACE_N, ACE_S and NE regions were also shown. The depth of mixed layer is shown as red line.

Figure 5: The relationship of a) Chl-a and POC, b) Chl-a and PN, c) Salinity and POC, d) salinity and PN, e) POC and $\delta^{13}\text{C}_{\text{POM}}$ and f) PN and $\delta^{15}\text{N}_{\text{POM}}$ in the mixed layer.

Figure 6: Relationship between depth of nitracline and $\delta^{15}\text{N}_{\text{POM}}$ in the mixed layer. The regression line and equation were also shown.

Figure 1

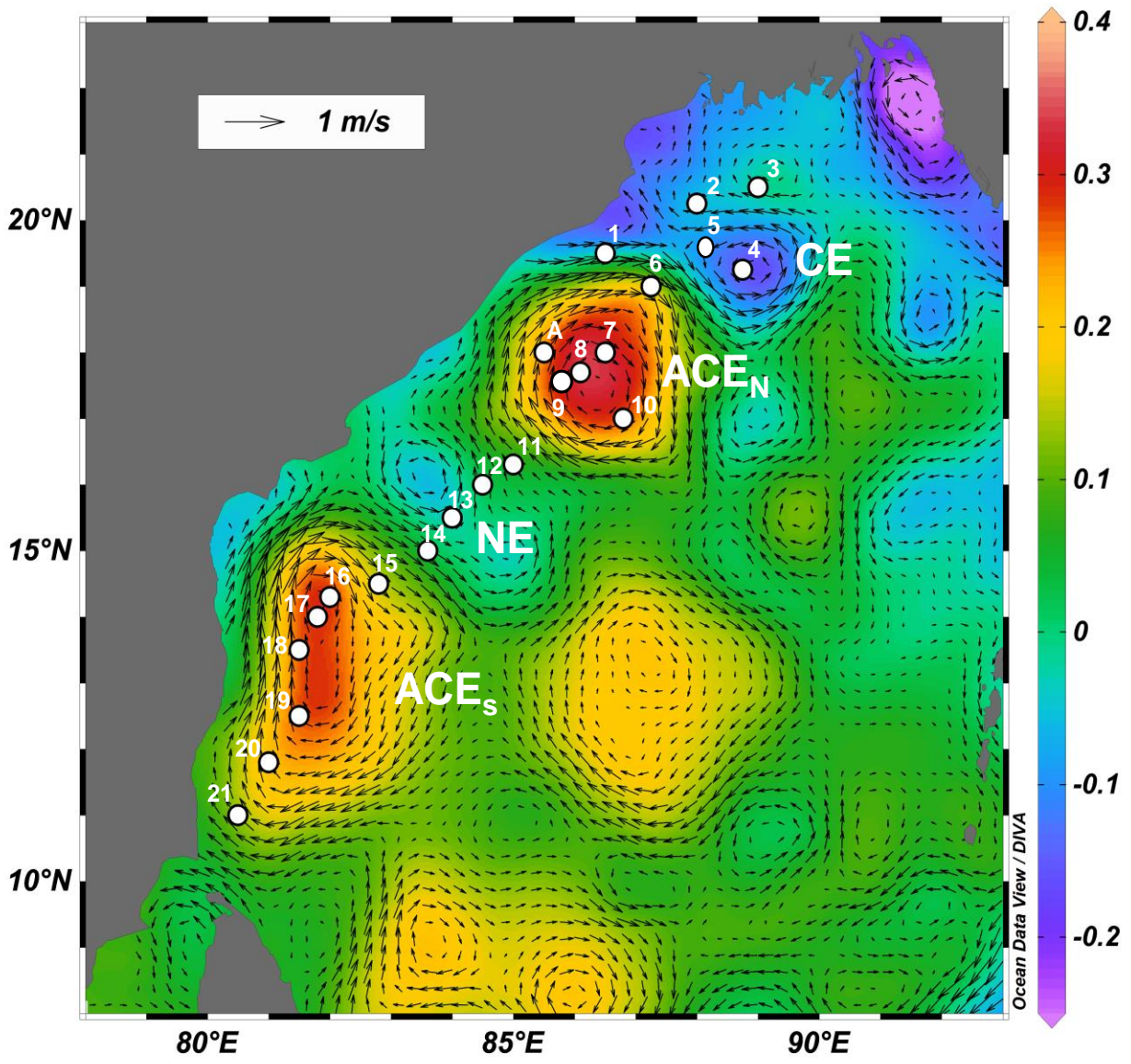


Figure 2

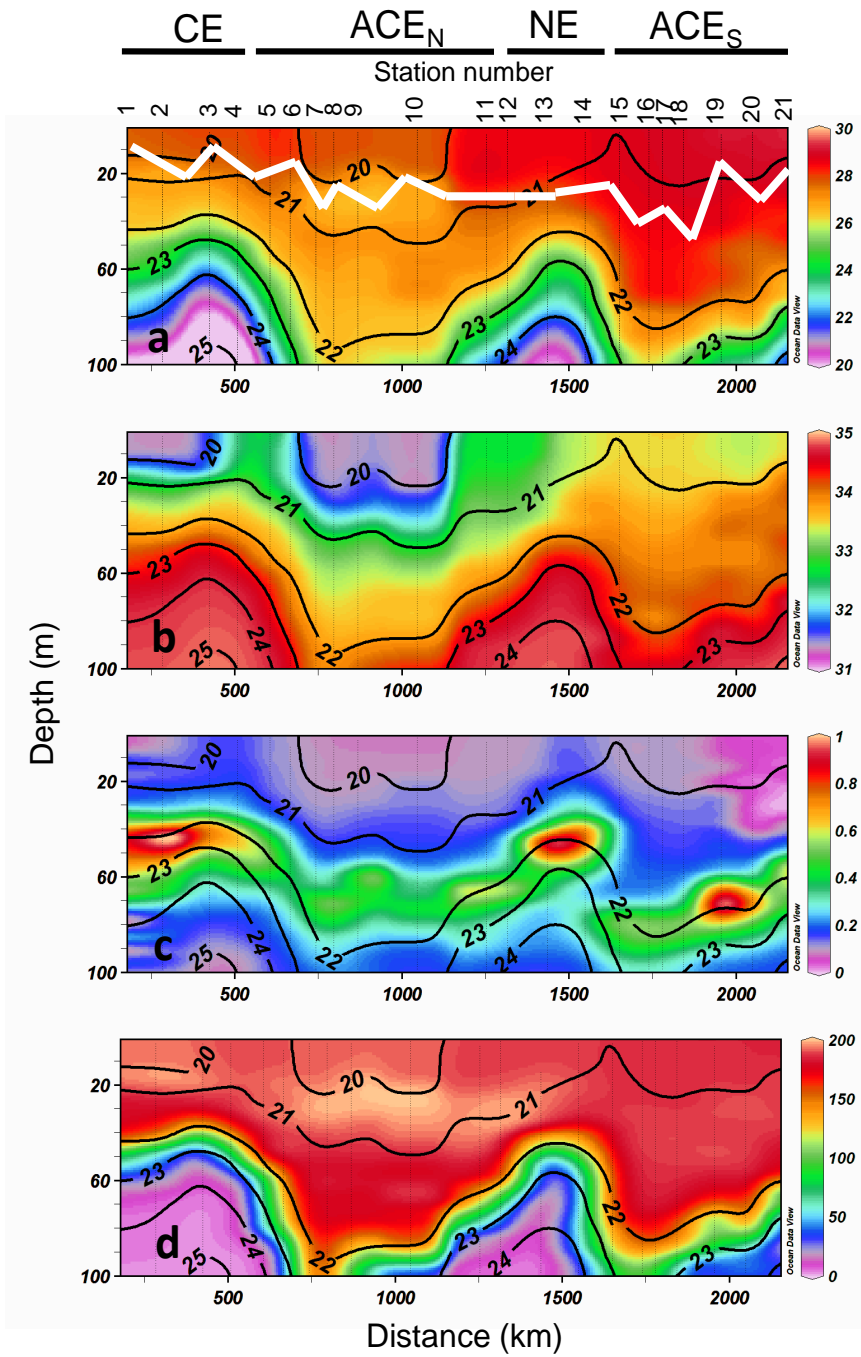


Figure 3

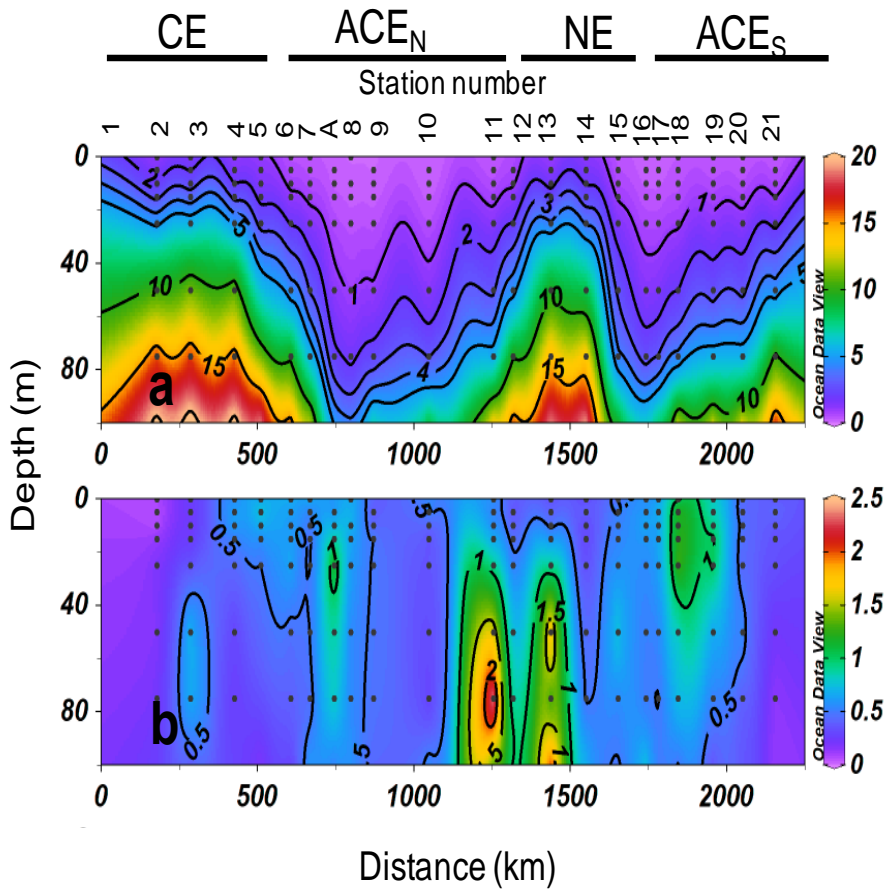


Figure 4

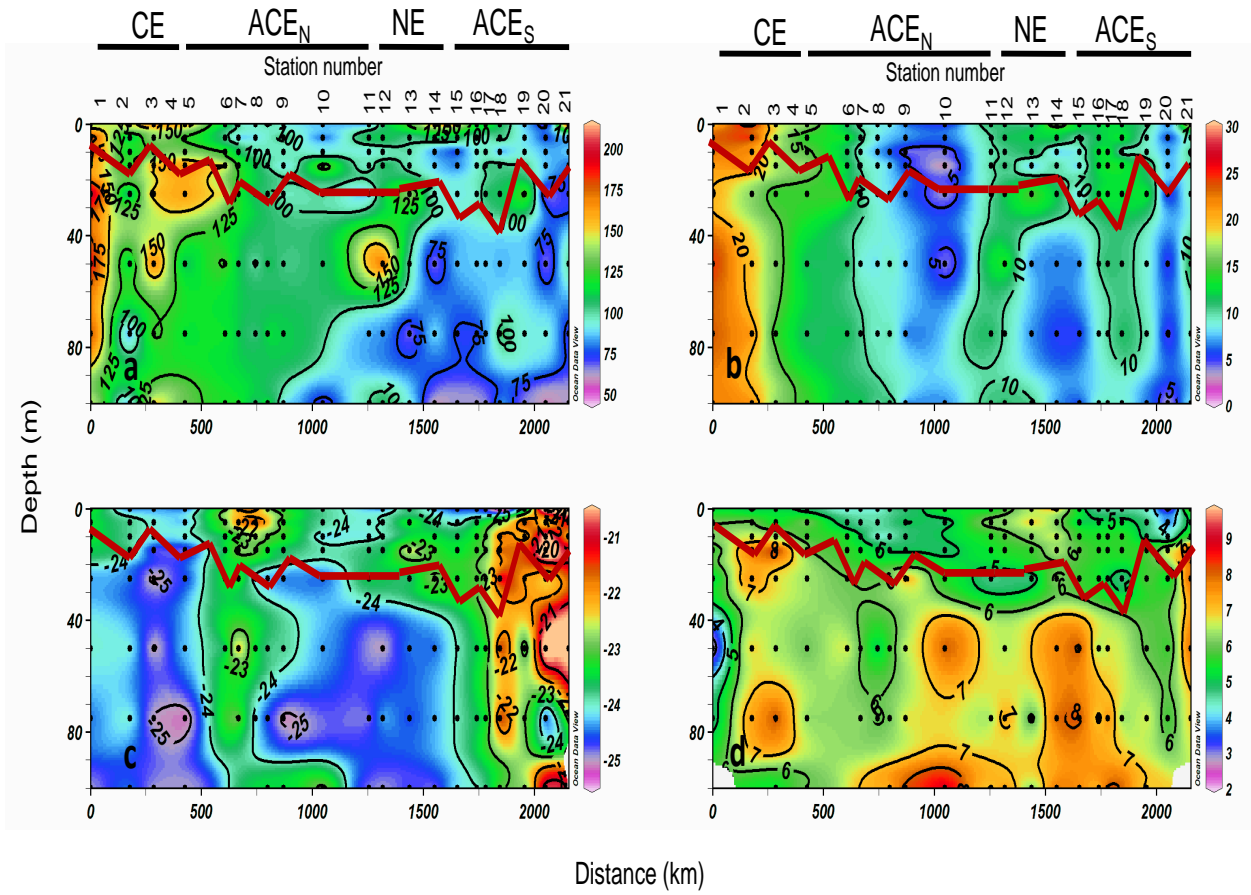


Figure 5

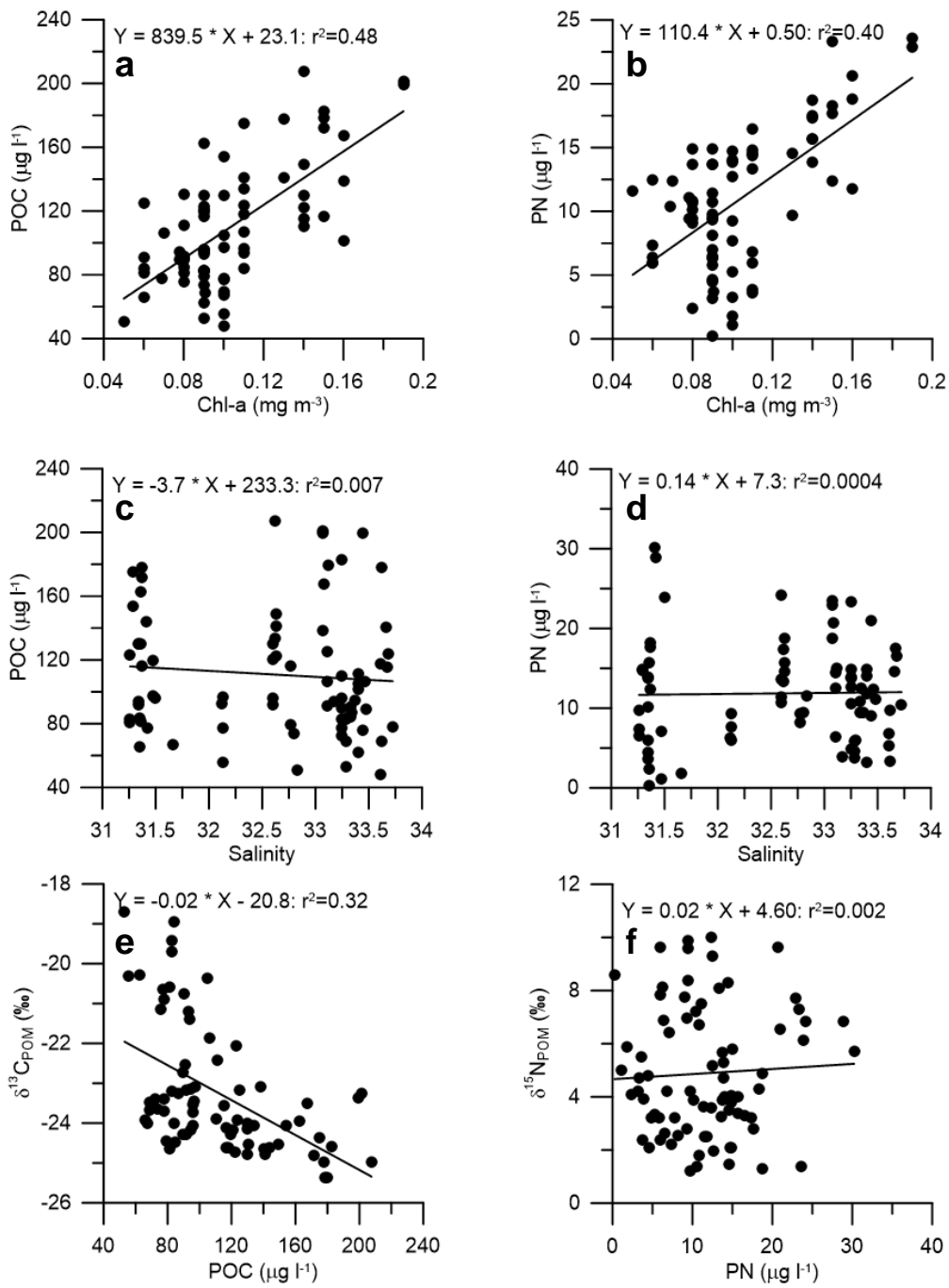
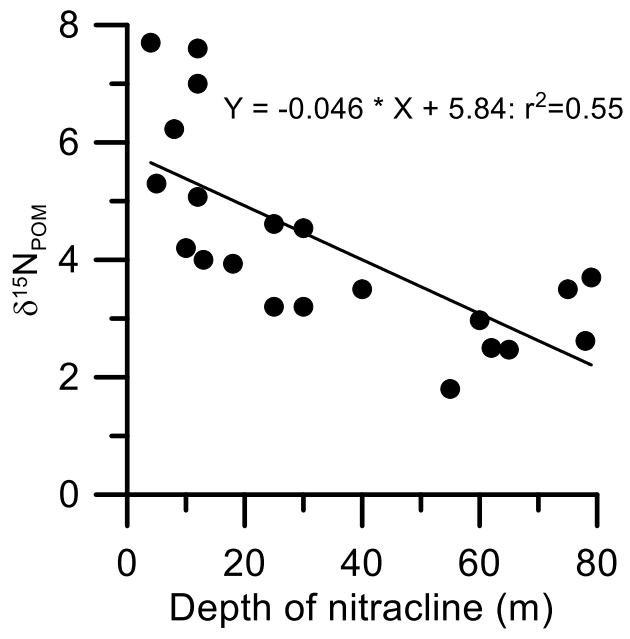


Figure 6



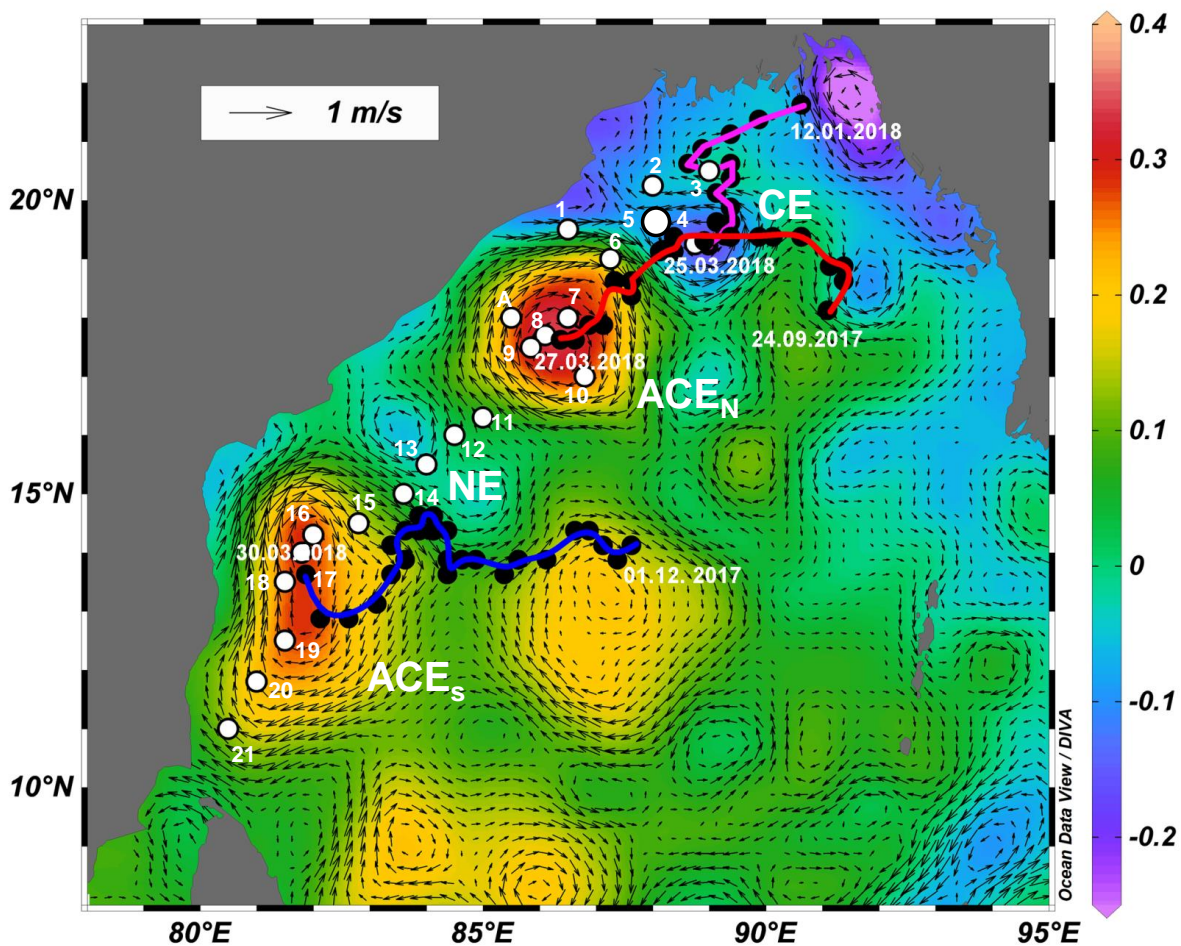
Role of eddies on organic matter production and f-ratios in the Bay of Bengal

V.V.S.S. Sarma^{1,2*}, K. Yadav¹, S. Behera^{1,2}

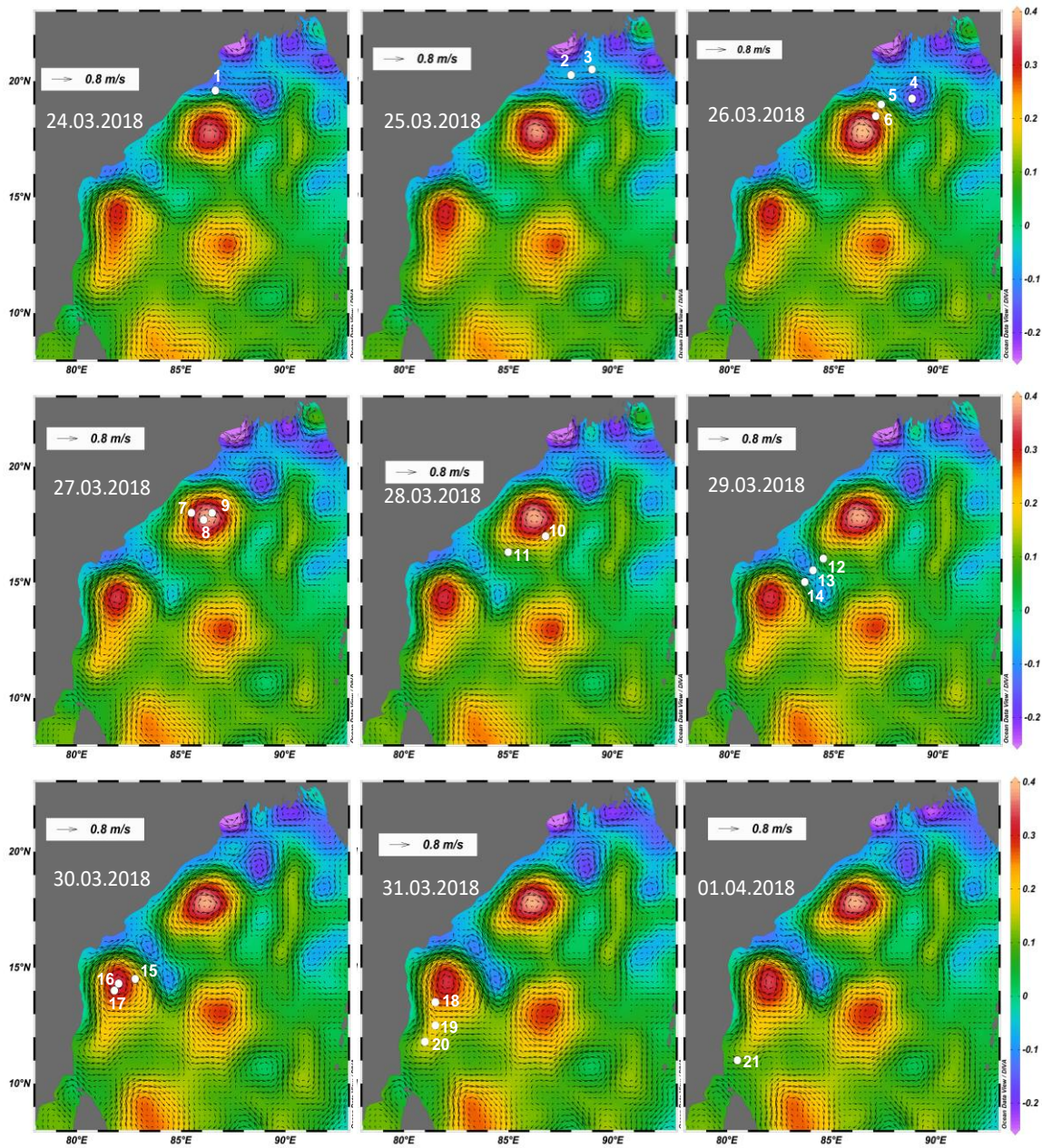
¹CSIR-National Institute of Oceanography, Regional Centre, Visakhapatnam, India

²Academy of Scientific and Innovative (AcSIR), CSIR-National Institute of Oceanography, Dona Paula, Goa, India

Supplementary Figure S1: The study region with station locations. The back ground shows the SSHA (color scale), surface geotrophic currents directions and speed are shown as arrows. The track of sampled eddies are also shown based on daily SSHA data analysis (CE=purple, ACE_N=red and ACE_S= blue). The date of formation of each eddy and sampling dates are also given. Location of stations (white circles) and their numbers are also given.



Supplementary Figure S2: The SSHA (color scale) and surface currents directions (arrows) on the day of collection. The white dots and number indicates station location and its number (as per Figure 1) are also shown.



Supplementary Figure S3: Spatial distribution of N^* (μM) along the cruise track in the study region.

